

## Self-assembled hexagonal Au and Ag particle networks on silicon from Au and Ag nanoparticle solutions

P. Y. Su, M. Y. Lu, J. M. Liang\*, M. Y. Lin, J. C. Hu, S. L. Cheng and L. J. Chen

Department of Material Science and Engineering, National Tsing Hua University, Hsinchu, Taiwan, Republic of China

Fax: +886-3-5718328, e-mail: ljchen@mse.nthu.edu.tw

\*National Nano Device Laboratories, Hsinchu, Taiwan, Republic of China

Fax: +886-3-5713403, e-mail: jamesliang@ndl.gov.tw

Self-assembled hexagonal Au and Ag particle networks, on silicon have been achieved by a simple method. Honeycomb structures of Au and Ag nanoparticles on silicon were drop-cast from the Au and Ag nanoparticle solution. Hexagonal networks with discrete Au and Ag particles were generated in samples annealed in N<sub>2</sub> ambient. As the cell size can be adjusted by the tuning of the deposition conditions, the scheme promises to be an effective patterning method without complex lithography.

Key words: self-assembly, nanoparticles, lithography

### 1. Introduction

Nanoparticles of Au and other noble metals are attracting much attention because of their potential applications in microelectronics [1,2]. Well-ordered arrays of metal nanoparticles represent an exciting new class of materials, which provide opportunities for optimizing materials properties and offer possibilities for probing a new and potential collective phenomenon [3]. Many two-dimensional (2-D) arrays of metal nanoparticles by self-assembly were successfully formed. Self-assembly is herein defined as the autonomous organization of components into patterns or structures without artificial intervention [4]. In addition, small-sized Au catalyst has attracted increasing interest because of the discovery of extraordinary catalytic activity and specificity [5,6]. Using Au nanoparticles, consisting of metal inner-core and organic outer-shell, the nanostructured catalysts can be acquired taking into consideration of size controllability, monodispersity, processibility, and aggregation resistivity [7]. Au catalytic ability is connected to the controllable activation of the core-shell nanostructure or removal or reconstitution of the shell components. By using self-assembled colloidal polystyrene latex as a mask, nanosphere lithography (NSL) method has shown the promise to replace the traditional photolithography and electron beam lithography (EBL) [8]. Optical detection and spectroscopy of single molecules and single Ag nanoparticles have been achieved at room temperature with the use of surface-enhanced Raman scattering. The intrinsic Raman enhancement factors were on the order of  $10^{14}$  to  $10^{15}$ , much larger than the ensemble-averaged values derived from conventional measurements [9].

In an effort to grow larger-area hexagonal superlattice of Au and Ag nanoparticles on silicon from Au and Ag nanoparticle solutions, honeycomb structures with Au and Ag skeleton was observed to form. With appropriate annealing scheme, extraordinarily large in extent, regular hexagonal networks of Au and Ag particles were formed. In this paper, we report the self-assembly of hexagonal networks of Au and Ag

particles from Au and Ag nanoparticle solutions, respectively, as well as its underlying mechanism and technical implications.

### 2. Experimental procedures

The colloidal Au nanoparticles were synthesized by a two-phase method [10]. In order to achieve the highly regular patterns of Au nanoparticle [11], Au@TOAB-DT nanoparticles (TOAB: tetraoctylammonium bromide, DT: dodecanethiol) with narrow size distribution, formed by a displacement reaction of the outer-shells from TOAB to DT molecules, were used [12]. On the other hand, Ag@DT nanoparticles were synthesized without the displacement reaction since Ag@TOAB nanoparticles tended to agglomerate severely. Dispersion solutions of Au and Ag nanoparticles were prepared with 5.36 and 5 g of nanoparticles/liter (g/l) of toluene, respectively. A 20- $\mu$ l droplet of each dispersive solution of nanoparticles was drop-cast with a micro-pipet on a 5 mm x 5 mm n-type (001)Si wafer. The solvent was evaporated while placing the substrate in an air-extracting apparatus with appropriate airflow, humidity and temperature. The evaporation normally takes less than 10 min to complete. Heat treatments were carried out in a three-zone diffusion furnace in N<sub>2</sub> ambient. The nanoparticle microstructures were examined with a field emission scanning electron microscopy using a JEOL JSM-6500F FESEM operating at 15 keV acceleration voltage. In addition, a JEOL-2010 TEM operating at 200 keV in conjunction with an energy dispersion spectrometer (EDS) was utilized to examine the microstructures and determine the chemical composition.

### 3. Results and discussion

The displacement reaction has utilized both superior size and shape control of Au@TOAB nanodots and uniform dispersion capability of Au@DT nanodots to achieve an extraordinarily large in extent (3  $\mu$ m x 3  $\mu$ m) regular nanodot lattice structure. An example is shown in Fig. 1. The average size of the Au@TOAB-DT

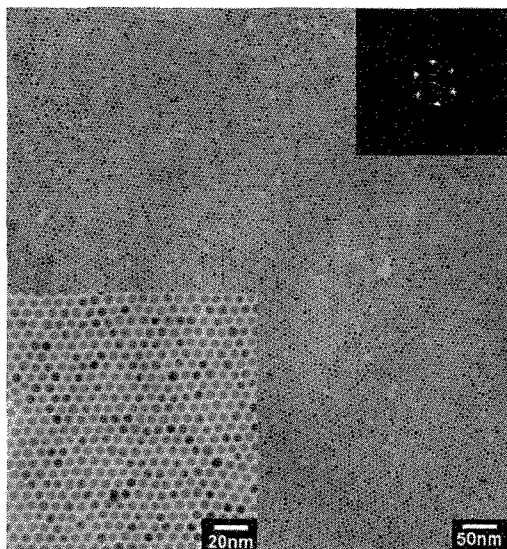


Fig. 1 TEM image of Au@TOAB-DT nanoparticle superlattice showing a long-range ordered and uniform in size 2-D array structure. Lower left inset is a magnified view of the selected region of the superlattice. Upper right inset is the FFT pattern of the selected area.

nanodots was 4.9 nm. The formation of the more uniform in size and regularly rounded Au@TOAB-DT nanodots can be attributed to the rapid displacement from TOAB to DT molecules in the outer-shells at room temperature. As a result, further growth of the inner-core Au nanodots was hindered [13]. As more Au nanodots were precipitated on the silicon substrate, intrigue patterns of circles, islands, labyrinthine and polygons were formed [14-16]. The cellular structures were observed in a wide variety of physical, biological, and ecological systems [17-21]. For instances, striking circular, labyrinthine, polygonal, and striped patterns of stones and soil were found in many polar and high alpine environments [21].

Regular hexagonal network was found to form in drop-cast samples by self-organization with a wide range of conditions. An example is shown in Fig. 2. For 5.36 g/l Au nanoparticles deposited samples annealed at 400 °C for 60 min, the integrity of honeycomb networks

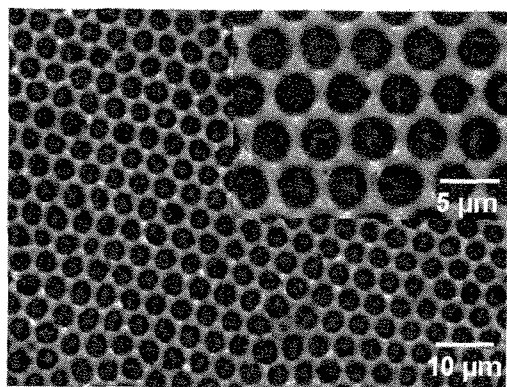


Fig. 2 SEM image of a 5.36 g/l Au nanoparticles deposited sample. The inset shows magnified view of selected area.

was still maintained. However, the ribbons of honeycomb networks were found to thin down as well as to become disconnected. An example is shown in Fig. 3. The inset shows magnified view of one of the hexagons. At this annealing temperature, the original core-shell structure of Au nanoparticles is expected to disintegrate since the organic shells were shown to be unstable at 140-330 °C [22,23]. After annealing at 800 °C for 1 h, the ribbons of honeycomb start to aggregate to the intersection which is attributed to the coarsening of Au structure driven by minimizing the total surface energy.

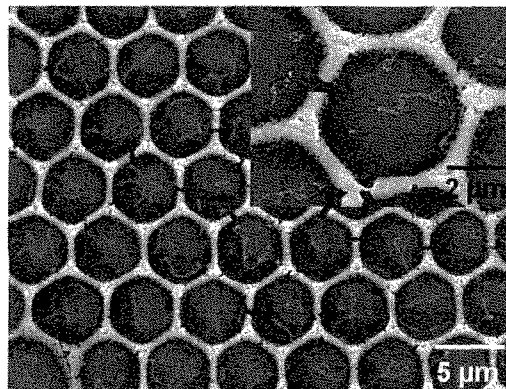


Fig. 3 SEM image of 5.36 g/l Au nanoparticles deposited sample annealed at 400 °C for 60 min. The inset shows magnified view of one of the hexagons.

As the annealing temperature was increased to 1000 °C for 60 min, Au atoms from hexagonal skeleton aggregated further at the intersections. If the samples were annealed in two steps, i.e. annealing at 400 °C for 1 h followed by annealing at 1000 °C for 1 h, extraordinarily large in extent and regular hexagonal Au network was observed to form. An example is shown in Fig. 4. It is thought that the low temperature annealing serves to release the voids and/or bubbles induced by the evaporation of organic compound at the outer shell. As a result, more regular polyhedral Au particles were formed after the second and high temperature annealing. On the other hand, the less orderly release of bubbles and/or voids in the samples heated directly at a temperature as high as 1000 °C may lead to less regular in shape Au particles at the intersections.

The eutectic point for the Au-Si system is known to be as low as 363 °C. XTEM images revealed the presence of a thin layer of oxide at the Au/Si interface and relatively small Au particles as shown in Fig. 5. We note that large Au particles were prone to be removed owing to the poor adhesion during the XTEM sample preparation. The oxide layer at the Au/Si is likely to be induced by the reaction of a small amount of oxygen in the annealing ambient and/or outer-shell of Au nanoparticles with silicon. The oxide interlayer stabilized the Au particles so that the mixing of Au with Si and rapid diffusion into the underlying Si are prevented. As a result, the positioning of Au particles at the intersections of hexagonal walls is maintained.

The formation of hexagonal networks has often been attributed to the Benard-Marangoni instabilities, which refers to the phenomenon that liquid flows along a gas-liquid or a liquid-liquid interface from areas

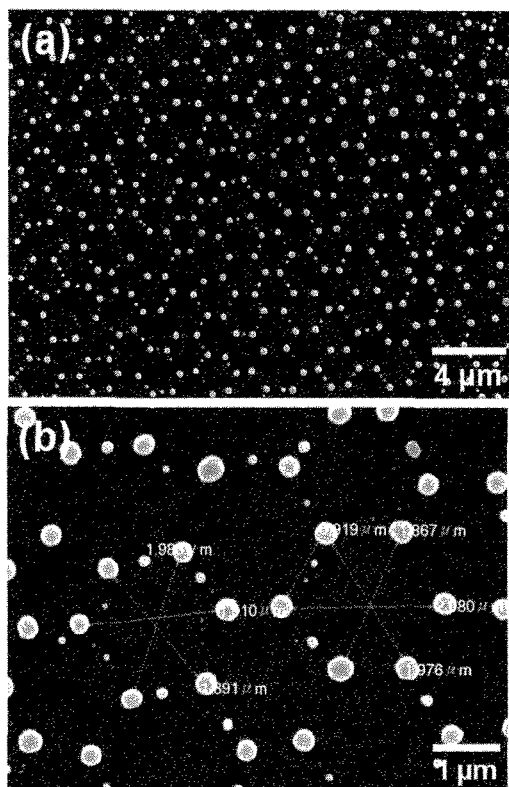


Fig. 4 (a) SEM image of 5.36 g/l Au nanoparticles deposited sample annealed at 400 °C, then 1000 °C each for 60 min, (b) magnified view of selected area in (a).

having low surface tension to areas having higher surface tension [24], of deposited liquid films. On the other hand, Shah et al. showed that water droplets condense on the evaporating dispersion and self-organize into an ordered array that templates the deposition of hydrophobic nanocrystals [25]. In the present study, with the aid of video imaging under an optical microscope, it was observed unequivocally that the hexagonal network was formed from the condensation of water droplets, arranged in hexagonal form, from the air moisture. The critical role played by the moisture is reflected in the requirement of relatively high humidity in the ambient to facilitate the growth of the regular networks.

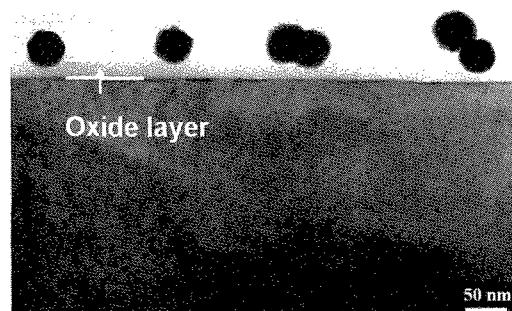


Fig. 5 XTEM image showing the presence of a thin layer of oxide at the Au/Si interface.

The present results showed that regular honeycomb patterns of Au nanoparticles formed at room temperature can be translated to hexagonal networks after 1000 °C annealing without complex lithography. As Au is known to be an excellent catalyst for a number of applications, it would be of great interest to explore further the positioning of catalyzing dots. The control of the particle size and the spacing is of critical challenges. It is worthwhile to note that some applications such as photonics, catalysis and sensors require organization into more spatially complex macroporous structures where the lattice parameter is on the order of micrometer or more [26].

Figure 6 shows the FESEM images of Ag networks after annealing at different temperatures. With increasing the annealing temperature, the ribbons of honeycomb aggregate to the intersection gradually. The phenomenon is rather similar to the formation of Au

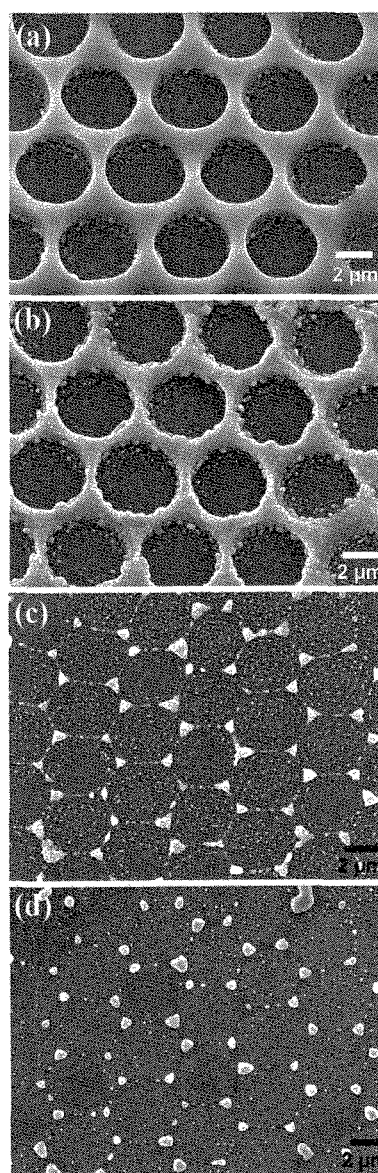


Fig. 6 SEM images of Ag networks (a) as-deposited and after annealing at (b) 400 °C, (c) 600 °C and (d) 700 °C for 60 min.

networks.

To control the size of cellular network, the concentration of Au solution, evaporation rate of toluene and substrate temperature were varied. Regular networks were observed to form under appropriate conditions. For example, at the highest concentration (5.36 g/l) studied, regular honeycomb networks were observed to cover almost the whole area (5 mm x 5 mm) of the samples. The networks consist of ribbons of nanoparticles with an average diameter of 5.2  $\mu\text{m}$ . As the concentration was lowered (1 g/l), the average diameter of networks increases to 6.5  $\mu\text{m}$ . The change is correlated to the faster evaporate rate for the sample of lower concentration [26]. Keeping the supersaturation of water moisture as the predominant factor in forming the regular network in mind, the size of network can be controlled to vary from 2 to 12  $\mu\text{m}$  by varying the solute concentration, evaporation rate and substrate temperature. For examples, with 5.36 g/l solution, ambient pressure of 700 mmHg and substrate temperature 20  $^{\circ}\text{C}$ , the cell sizes fall within the range of 2.5-3  $\mu\text{m}$ . On the other hand, as the substrate temperature was maintained at 2  $^{\circ}\text{C}$  and other conditions being identical, the cell sizes increase to 10-10.5  $\mu\text{m}$ .

#### 4. Conclusions

In summary, highly regular hexagonal Au and Ag particle networks were formed by annealing the hexagonal cells on silicon. The cells were generated from the drop-cast of Au and Ag nanoparticle solutions. Two-step annealing, i.e. annealing at 400  $^{\circ}\text{C}$  followed by annealing at 1000  $^{\circ}\text{C}$  for 1 h each was found to be effective to improve the regularity of the Au particle network. The Au cells were found to be induced by the drying of water droplet arrays condensed on the Au solution. In annealed samples, Au atoms aggregate to the intersections of hexagonal skeletons. The presence of a thin oxide layer at the Au/Si interface stabilizes the Au particles at the intersections at a temperature as high as 1000  $^{\circ}\text{C}$ . Similar phenomenon of the formation of Ag networks to that of Au networks was observed.

#### 5. Acknowledgment

The research is supported by the Republic of China National Science Council grant No. NSC 91-2215-E-007-002 and Ministry of Education grant No. 91-E-FA04-1-4.

#### 6. References:

- [1] G. Schmid, Chem. Rev., **92**, 1709 (1992).
- [2] R. P. Andres, J. D. Bielefeld, J. I. Henderson, D. B. Janes, V. R. Kolagunta, C. P. Kubiak, W. J. Mahoney and R. G. Osifchin, *Science*, **273**, 1690 (1996).
- [3] C. Renard, C. Ricolleau, E. Fort, S. Besson, T. Gacoin, and J. P. Boilot, *Appl. Phys. Lett.* **80**, 300 (2002).
- [4] G. M. Whitesides and B. Grzybowski, *Science* **295**, 2418 (2002).
- [5] M. Haruta, *Catal. Today* **36**, 153 (1997).
- [6] M. Valden, X. Lai and D. W. Goodman, *Science* **281**, 1647 (1998)
- [7] M. M. Maye, W. X. Zheng, F. L. Leibowitz, N. K. Ly and C. J. Zhong, *Langmuir* **16**, 490 (2000).
- [8] C. L. Haynes and R. P. Van Duyne, *J. Phys. Chem. B*, **105**, 5599 (2001).
- [9] S. Nie and S.R. Emory, *Science* **275**, 1102 (1997).
- [10] J. Fink, C. J. Kiely, D. Bethell, D. J. Schiffrin, *Chem. Mater.* **10**, 922 (1998).
- [11] C. Stowell and Brian A. Korgel, *Nano Lett.* **1**, 595 (2001)
- [12] J. C. Hu, P. Y. Su, V. Lapeyronie, S. L. Cheng, M. Y. Lin, and L. J. Chen, unpublished work.
- [13] T. Teranishi, S. Hasegawa, T. Shimizu, and M. Miyake, *Adv. Mater.* **13**, 1699 (2001).
- [14] M. Maillard, L. Motte, A. T. Ngo, and M. P. Pileni, *J. Phys. Chem. B* **104**, 11871 (2000).
- [15] G. Reiter, *Phys. Rev. Lett.* **87**, 186101-1 (2001).
- [16] P. Moriarty and M. D. R. Taylor, *Phys. Rev. Lett.* **89**, 248303-1 (2002).
- [17] D. Weaire and N. Rivier, *Contemp. Phys.* **25**, 59 (1984).
- [18] J. Stavans, *Rep. Prog. Phys.* **56**, 733 (1993).
- [19] J. A. Glazier and D. Weaire, *J. Phys. Condens. Matter* **4**, 1867 (1992).
- [20] B. Levitan and E. Domany, *Int. J. Mod. Phys. B* **10**, 37 (1996)
- [21] M. A. Kessler and B. T. Werner, *Science* **299**, 380 (2003)
- [22] J. Luo, V. W. Jones, M. M. maye, L. Han, N. N. Kariuki, and C. J. Zhong, *J. Am. Chem. Soc.* **27**, 13988 (2002)
- [23] J.N. O'Shea, M.A. Philips, M.D.R. Taylor, P. Moriarty, M. Brust, and V.R. Dhanak, *Appl. Phys. Lett.* **81**, 5039 (2002)
- [24] H. Benard, *Rev. Gen. Sci. Pur. Appl.* **11**, 1261 (1900)
- [25] P.S. Shah, M.B. Sigman, Jr. C.A. Stowell, K.T. Lim, K.P. Johnston, and B.A. Korgel, *Adv. Mater.* **15**, 971 (2003).
- [26] A. Oron and S. G. Bankoff, *J. Colloid Interface Sci.* **218**, 152 (1999).

(Received October 13, 2003; Accepted November 28, 2003)